(20) C. S. Wright, J. Mol. Biol., 67, 151 (1972); J. D. Robertus, J. Kraut, R. A. Alden, and J. J. Birktoft, Biochemistry, 11, 4293 (1972).
(21) M. S. Natta and D. D. Staley, J. Biol. Chem., 249, 732 (1974).
(22) J. B. Greenstein and M. W. Winitz, "Chemistry of the Amino Acids", Wiley, New York, 1961, pp 1266–1271 and 2173–2174.
(23) J. de Jersey, M. T. C. Runnegar, and B. Zerner, Biochem. Biophys. Res. Commun., 25, 383 (1966).
(24) D. F. DeTar, R. Silverstein, and F. F. Rogers, J. Am. Chem. Soc., 88, 1024 (1966).
(25) E. Mohr and H. Stroschein, Chem. Ber., 42, 2521 (1909).
(26) F. M. F. Chen, K. Kuroda, and N. L. Benolton, Synthesis, 230 (1979).
(27) M. Bergmann, F. Stein, and C. Witte, Justus Liebigs Ann. Chem., 449, 227 (1926).
(28) G. R. Schonbraum, B. Zerner, and M. L. Bender, J. Biol. Chem., 236, 2930 (1961); M. L. Bender et al., J. Am. Chem. Soc., 88, 5890 (1966).
(29) Because of the large $[\alpha]_D$ values of the cyclodextrins, a contamination of 5% in a completely racemic sample of acylamino acid would lead to an erroneous attribution of an enantiomeric excess between 15 and 50% depending on the substrate.
(30) S. Moore, J. Biol. Chem., 243, 6281 (1968).
(31) R. H. Wightman, J. Staunton, and A. R. Bathersby, J. Chem. Soc., Perkin Trans. 1, 2355 (1972).
(32) C. T. Walsh, A. Schonbrunn, and R. Abeles, J. Biol. Chem., 246, 6855 (1971).

23672 RP, a New Macrolide Antibiotic from *Streptomyces chryseus*. Mass Spectrometry Study and X-ray Structure Determination

Bernadette Arnoux,*[1a] Claudine Pascard,*[1a] Laurent Raynaud,[1b] and Jean Lunel[1b]

Contribution from the Institut de Chimie des Substances Naturelles, CNRS, 91190 Gif sur Yvette, France, and Rhône-Poulenc Industries, Recherches et Développement, Centre Nicolas Grillet, 94400 Vitry, France. *Received August 27, 1979*

Abstract: A new macrolide antibiotic, 23672 RP, has been isolated from *Streptomyces chryseus* DS 12370 (NRRL 3892). It has some activity in vitro and in vivo against mycobacteria. Structural studies have been run by mass spectrometry and X-ray crystallography, the complete structure being established by the latter technique. 23672 RP has a 14-membered lactonic ring resembling that of lankamycin. Three sugar units are bonded to C-3, C-5, and C-15, and an α-hydroxyisovalerate chain is linked to C-11.

In the course of the research of new antimicrobial agents, 23672 RP was isolated from the culture broth of *Streptomyces chryseus* DS 12370 (NRRL 3892). This compound is a neutral macrolide according to its physical and chemical properties. It is atoxic in the mouse at the dose of 2.5 g/kg when administered by subcutaneous route, and it has some activity in vitro and in vivo against Gram-positive bacteria and mycobacteria without any detectable activity against Gram-negative bacteria. The following minimum inhibitor concentrations were determined (μg/mL): *Staphylococcus aureus* ATCC 6538P, 0.54; *Sarcina lutea* ATCC 9431, 0.07; *Bacillus cereus* ATCC 6630, 0.10; *Mycobacterium* species ATCC 607, 0.42; *Mycobacterium* H37Rv, 1.25; *Escherichia coli* ATCC 9637, >200. The compound is effective in protecting mice from lethal infections produced by staphylococci; the curative doses (CD_{50} values) in mice are 35 and 85 mg/kg by subcutaneous and per os routes, respectively. Against a mycobacterial infection by virulent human strain, the compound at the doses of 100–200 mg/kg by subcutaneous or per os routes increases significantly the life of treated animals comparatively to the reference.[2] We wish to report here studies on this compound by mass spectrometry and X-ray crystallography, the structure being established by the latter technique.

Experimental Section

A. Mass Spectrometry. 23672 RP has been studied by field desorption, chemical ionization, and electron impact mass spectrometry.

Field Desorption. Spectra have been carried out on a Varian MAT 311A apparatus by the cationization technique upon addition of potassium iodide. The result is given in Figure 1 with the peak at M + K 1017: M = 978. The three major fragments are *m/e* 129, 145, and 175.

Chemical Ionization. Spectra have been recorded on a Finnigan 4000 processed by the Data System 6100, using isobutane as reactant gas. The chemical ionization mass spectrum of 23672 RP is reproduced in Figure 2. The protonated molecular ion (MH^+) gives the peak at *m/e* 979; the prominent peaks in the low-mass portion of the spectrum correspond to fragment ions of the sugar residues at *m/e* 129, 145, and 175.

Electron Impact. The spectrum has been recorded on Finnigan 3300 and AEI MS50 apparatus, this last one processed by the Data System DS 50. Not unexpectedly, 23672 RP does not display a detectable molecular ion; the peak of highest mass occurs at *m/e* 689. Some of the fragments have been measured exactly in order to establish the formula at *m/e* 129, 145, and 175. Three sugars have been displayed in the form of oxonium ions: 129.0550, oxonium ion $C_6H_9O_3$, sugar $C_6H_{10}O_4$; 145.0875, oxonium ion $C_7H_{13}O_3$, sugar $C_7H_{14}O_4$; 175.0998, oxonium ion $C_8H_{15}O_4$, sugar $C_8H_{16}O_5$. The two last sugars may correspond to mycarose and mycinose.

B. X-ray Diffraction. Experimental. The sample of 23672 RP was crystallized from an aqueous acetone solution. Crystals belong to the monoclinic space group $P2_1$; the unit cell dimensions are a = 11.147 (3) Å, b = 18.350 (4) Å, c = 14.564 (4) Å, β = 93.59 (5)°, Z = 2.

A crystal with approximate dimensions 0.33 × 0.38 × 0.41 mm was mounted on a Philips PW1100 four-circle diffractometer. Intensity data were collected by the use of Ni-filtered Cu radiation, up to 2θ = 136°. Background was estimated from measurements outside reflections between θ = 2° and θ = 66°; 3888 integrated intensities out of 5530 independent reflections were above $3\sigma(I)$, where $\sigma(I)$ is the standard deviation derived from counting statistics. No absorption correction was applied.

Structure Determination and Refinement. The structure was solved by direct methods. The starting set was formed with three reflections fixing the origin, and six symbols which were chosen in Σ_2[3a] and positive quartets[3b] listings as reflections having the more numerous interactions. This set has been tested with Riche's phase function,[4] but too many solutions appeared. The four well-defined symbols were selected in a multisolution program,[5] in which the phases were generated by the magic integers procedure,[6] and where the solutions are ranked according to the NQ test[3b] and residual.[7] This procedure was not sufficient to provide the solution. We then added two Σ_1 relations[3a] in the starting set. This time, the set with the minimal R and the more negative NQ value led to the solution.

0002-7863/80/1502-3605$01.00/0

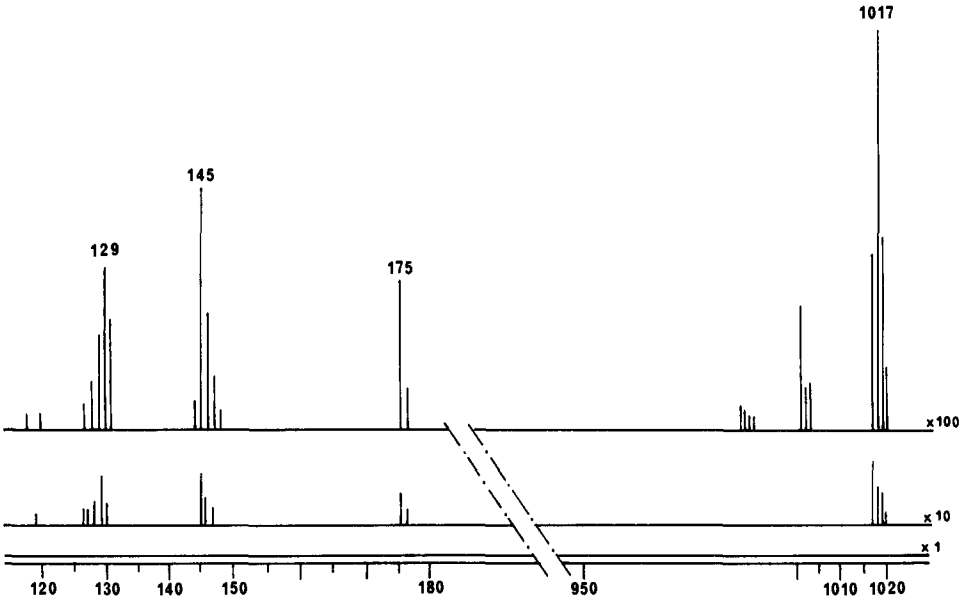

Figure 1. Field desorption mass spectrum of 23672 RP.

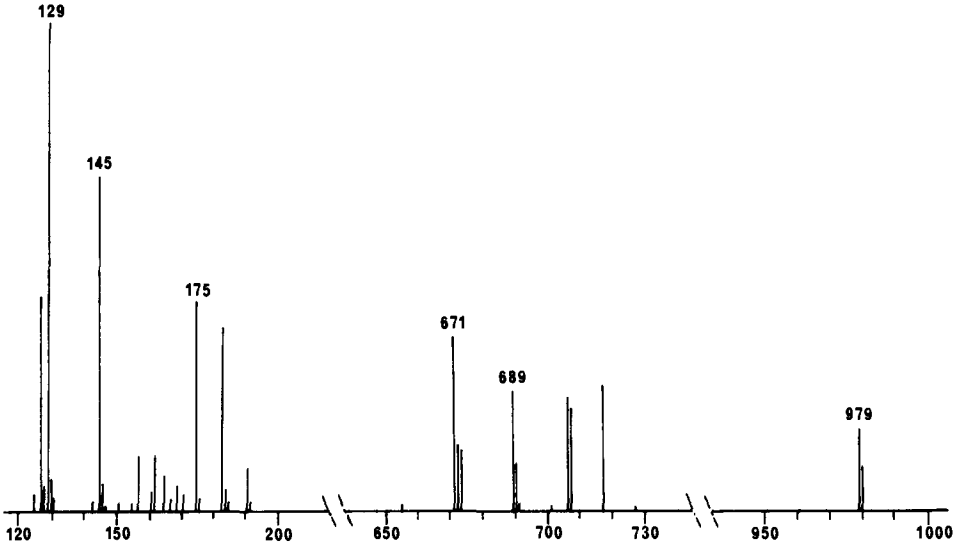

Figure 2. Chemical ionization mass spectrum of 23672 RP.

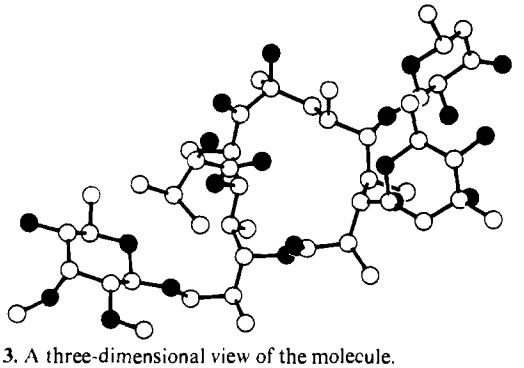

Figure 3. A three-dimensional view of the molecule.

The calculated E map revealed all the atoms of the macrocycle. The remaining three sugar units and the side chain were located on F_o Fourier synthesis. The identification of the hydroxyl group on the valerate chain (as well as the keto group on the third unknown sugar residue) was made according to classical bond lengths and angles and electronic density.

Block-diagonal least-squares refinement using individual isotropic temperature factors and a fractional weighting scheme reduced the R ($R = \Sigma||F_o| - |F_c||/\Sigma|F_o|$) value to 0.13. At this stage, a Fourier difference synthesis revealed two molecules of solvent, one of acetone and one of water. Hydrogen atoms which could be located theoretically (C-H, 1.0 Å; C-C-H, 109 or 120°) were introduced in the refinement procedure but not refined employing individual anisotropic temperature factors; 17 additional hydrogen atoms were located on difference syntheses, the total number of found hydrogen atoms amounting to 48. The refinement converged to $R = 0.080$. Coordinates of heavy atoms are given in Table I. A three-dimensional view of the molecule is shown in Figure 3, and the complete molecular formula is given in Figure 4.

Results

The structure resembles that of lankamycin[8] or kujimycin and corresponds to the correct formula: $C_{48}H_{82}O_{20}$.

A. Macrocycle Description. The macrocycle can be described according to Celmer's model.[9] The absolute configuration is as follows with that of lankamycin: this macrolide, 2*R*,3*S*,4*R*,5*S*,6*S*,8*S*,10*R*,11*S*,12*S*,13*R*,14*S*,15*S*; lankamycin, 2*R*,3*S*,4*R*,5*S*,6*S*,8*S*,10*R*,11*S*,12*R*,13*R*.

The main difference is the presence of the side chain α-hydroxyisovalerate ester bonded to C-11 which causes the reversal of configuration of C-12.

The general aspect of the molecule is that of a flattened

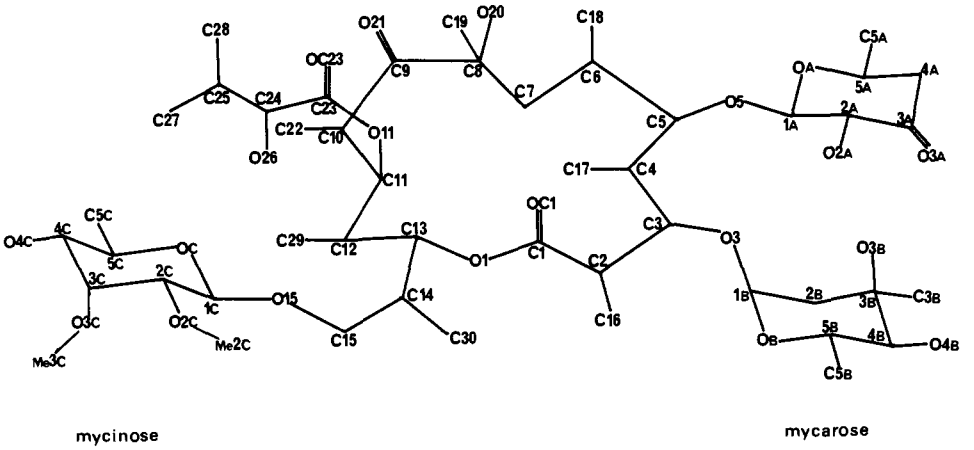

Figure 4. Formula of 23672 RP with the atomic numbering used in this study.

Table I. Atomic Coordinates ($\times 10^4$) with the esd's in Parentheses

atom	*x*	*y*	*z*	atom	*x*	*y*	*z*
O(1)	4188 (4)	−1998 (3)	−3249 (4)				
C(1)	4682 (7)	−1324 (6)	−3211 (7)	2(A)	5143 (8)	−977 (6)	2309 (7)
OC(1)	4356 (6)	−824 (4)	−3672 (5)	3(A)	5641 (12)	−528 (8)	3079 (9)
C(2)	5674 (7)	−1307 (5)	−2440 (6)	4(A)	4954 (12)	188 (9)	3162 (9)
C(3)	5309 (7)	−773 (5)	−1671 (7)	5(A)	4778 (10)	573 (7)	2252 (8)
C(4)	5066 (7)	−1164 (5)	−786 (7)	O2(A)	5928 (6)	−1570 (4)	2182 (5)
C(5)	4318 (7)	−678 (4)	−180 (6)	O3(A)	6502 (9)	−703 (6)	3602 (6)
C(6)	2982 (7)	−603 (4)	−501 (6)	C5(A)	3882 (16)	1245 (8)	2242 (12)
C(7)	2241 (6)	−1183 (5)	−86 (6)	O(3)	6257 (4)	−248 (3)	−1450 (4)
C(8)	830 (6)	−1209 (5)	−346 (6)	O(B)	5498 (5)	928 (3)	−1573 (4)
C(9)	507 (6)	−1246 (5)	−1385 (5)	1(B)	6205 (8)	413 (6)	−1963 (7)
C(10)	896 (7)	−1905 (4)	−1919 (6)	2(B)	7495 (8)	684 (5)	−2033 (6)
C(11)	1730 (7)	−1722 (4)	−2666 (5)	3(B)	8065 (7)	926 (5)	−1126 (6)
C(12)	2132 (7)	−2358 (4)	−3253 (6)	4(B)	7256 (8)	1486 (5)	−693 (7)
C(13)	3093 (6)	−2121 (5)	−3881 (5)	5(B)	5958 (7)	1203 (5)	−663 (6)
C(14)	3471 (7)	−2665 (5)	−4584 (6)	O3(B)	8215 (4)	289 (3)	−503 (4)
C(15)	2376 (7)	−3019 (5)	−5099 (6)	C3(B)	9350 (8)	1228 (5)	−1227 (8)
C(16)	6851 (8)	−1104 (9)	−2924 (10)	O4(B)	7671 (5)	1688 (3)	200 (5)
C(17)	6241 (7)	−1456 (5)	−258 (7)	C5(B)	5120 (9)	1819 (6)	−402 (9)
C(18)	2570 (8)	191 (5)	−358 (8)	O(15)	1730 (4)	−2430 (3)	−5557 (4)
C(19)	317 (7)	−1897 (5)	109 (6)	O(C)	−198 (4)	−2598 (3)	−5148 (4)
O(20)	287 (5)	−574 (3)	18 (4)	1(C)	560 (7)	−2648 (5)	−5895 (6)
O(21)	−121 (5)	−770 (3)	−1744 (4)	2(C)	140 (7)	−2109 (5)	−6652 (6)
C(22)	−264 (8)	−2278 (5)	−2316 (6)	3(C)	−1208 (8)	−2259 (5)	−6922 (6)
C(23)	1312 (9)	−507 (5)	−3228 (6)	4(C)	−1937 (7)	−2281 (5)	−6116 (6)
C(24)	349 (11)	−110 (6)	−3851 (9)	5(C)	−1415 (7)	−2831 (5)	−5399 (6)
C(25)	375 (12)	−305 (6)	−4845 (7)	O2(C)	794 (5)	−2143 (4)	−7444 (4)
O(26)	444 (9)	644 (5)	−3714 (6)	ME(2C)	1896 (9)	−1740 (7)	−7392 (7)
C(27)	1631 (13)	−126 (9)	−5190 (10)	O3(C)	−1276 (5)	−2952 (3)	−7396 (4)
C(28)	−650 (17)	105 (9)	−5420 (10)	ME(3C)	−1840 (9)	−2930 (7)	−8317 (6)
C(29)	2573 (8)	−3015 (5)	−2644 (7)	O4(C)	−3148 (5)	−2456 (4)	−6397 (4)
C(30)	4342 (8)	−2317 (7)	−5225 (7)	C5(C)	−2060 (8)	−2827 (7)	−4540 (7)
O(11)	1119 (4)	−1222 (3)	−3326 (4)	AC	7837 (10)	527 (6)	1531 (8)
OC(23)	2068 (6)	−211 (4)	−2745 (5)	AC(CO)	8831 (14)	141 (9)	1681 (10)
O(5)	4401 (5)	−966 (3)	769 (4)	AC(C1)	8760 (13)	−563 (9)	1882 (10)
O(A)	4216 (6)	66 (4)	1609 (5)	AC(C2)	9840 (13)	645 (8)	1572 (10)
1(A)	4969 (7)	−553 (5)	1447 (6)	W	6361 (6)	6075 (4)	3038 (5)

Table II. Torsion Angles (deg)

C(13)-O(1)-C(1)-C(2)	−172	C(6)-C(7)-C(8)-C(9)	−54
O(1)-C(1)-C(2)-C(3)	117	C(7)-C(8)-C(9)-C(10)	−64
O(C1)-C(1)-C(2)-C(3)	62	C(19)-C(8)-C(9)-O(21)	−118
C(1)-C(2)-C(3)-C(4)	−113	O(20)-C(8)-C(9)-O(21)	1
C(16)-C(2)-C(3)-O(3)	10	C(8)-C(9)-C(10)-C(11)	119
C(2)-C(3)-C(4)-C(5)	161	O(21)-C(9)-C(10)-C(22)	57
O(3)-C(3)-C(4)-C (17)	49	C(9)-C(10)-C(11)-C(12)	178
C(3)-C(4)-C(5)-C(6)	−74	C(22)-C(10)-C(11)-O(11)	−63
C(17)-C(4)-C(5)-O(5)	35	C(10)-C(11)-C(12)-C(13)	173
C(4)-C(5)-C(6)-C(7)	−90	O(11)-C(11)-C(12)-C(29)	169
O(5)-C(5)-C(6)-C(18)	−96	C(11)-C(12)-C(13)-O(1)	−71
C(5)-C(6)-C(7)-C(8)	178	C(29)-C(12)-C(13)-C(14)	−62
		C(12)-C(13)-O(1)-C(1)	116

Table III. Intermolecular Short Distances (Å)

O20(x, y, z)-O3B($1 + x, y, z$)	2.861
OC23(x, y, z)-W1($1 - x, \frac{1}{2} + y, 2 - z$)	2.986
O2A(x, y, z)-O4C($1 - x, y, 1 - z$)	2.774
O4C(x, y, z)-W1($1 + x, 1 + y, 1 + z$)	2.860
O3B-AC	3.052
O4B-AC	2.878

crown as shown by the ORTEP drawing and the torsion angle values (Table II).

B. Sugar Units. The configuration of the macrocycle being defined as above, the sugar units can be described as unit A, β-D-4,6-dideoxy-3-ketoallose; unit B, β-L-mycarose; unit C, β-D-mycinose.

C. Hydrogen Bonds, The two molecules of solvent in the cell (acetone and water) are linked to the sugar units by hydrogen bonds: acetone (AC) to unit B; water (W) to unit C (cf. Table III). There are no internal hydrogen bonds between the oxygen atoms of the macrocycle except perhaps between O3B-O4B (2.8 Å) (H(O3B)-O4B, 2.4 Å) and O20-O21 (2.6 Å) (H(O20)-O21, 2.4 Å); the two oxygen atoms are in the same plane (see Table III).

This work provides geometric data for the whole family of lankamycin-type antibiotics.

Supplementary Material Available: Listing of observed and calculated structural factors and the bond lengths and angles (20 pages). Ordering information is given on any current masthead page.

References and Notes

(1) (a) Institut de Chimie des Substances Naturelles. (b) Rhône-Poulenc Industries.
(2) French Patent 2 126 108 (Feb 25, 1971 and July 22, 1974, Société Rhône-Poulenc).
(3) (a) Hauptman, H.; Karle, J. *Acta Crystallogr.* **1956**, *9*, 635–651. (b) De Tita, G.; Edmonds, J. W.; Langs, D. A.; Hauptman, H. *Acta Crystallogr., Sect. A* **1975**, *31*, 472–479.
(4) Riche, C. *Acta Crystallogr., Sect. A* **1974**, *29*, 133–137.
(5) Riche, C., locally written program, 1978.
(6) Main, P. *Acta Crystallogr., Sect. A* **1977**, *33*, 750–757.
(7) Karle, J.; Karle I.L. *Acta Crystallogr.* **1966**, *21*, 849–859.
(8) (a) Keller-Schierlein, W.; Roncari, G. *Helv. Chim. Acta* **1964**, *47*, 78–103. (b) Egan, Richard S.; Martin, Jerry R. *J. Am. Chem. Soc.* **1970**, *92*, 4129–4130.
(9) Celmer, W. D. *J. Am. Chem. Soc.* **1965**, *87*, 1801–1802.

Iron–Ligand Stretching Band in the Resonance Raman Spectra of Ferrous Iron Porphyrin Derivatives. Importance as a Probe Band for Quaternary Structure of Hemoglobin

Hiroshi Hori and Teizo Kitagawa*

Contribution from the Department of Biophysical Engineering, Faculty of Engineering Science, Osaka University, Toyonaka, Osaka, 560, Japan, and the Institute for Protein Research, Osaka University, Suita, Osaka, 565, Japan.

Received November 1, 1979

Abstract: Resonance Raman spectra of ferrous iron picket-fence porphyrin [$Fe^{II}(T_{piv}PP)$] derivatives were observed for the oxy and deoxy states, both in solution and as a solid. The Fe(II)-N(2-MeIm) stretching mode of $Fe^{II}(T_{piv}PP)$(2-MeIm) was assigned by observing the frequency shifts upon the ^{54}Fe isotopic substitution (+3 cm^{-1}) and perdeuteration of 2-methylimidazole (2-MeIm) (−3 cm^{-1}). From the isotopic shifts the vibrational displacements of the Fe(II) ion and 2-MeIm perpendicular to the porphyrin plane were evaluated to be as large as 0.04_8 and 0.03_1 Å, respectively. For the iron protoporphyrin-2-methylimidazole complex [Fe^{II}(PP)(2-MeIm)], the Fe(II)-N(2-MeIm) stretching band was also observed at 206 cm^{-1} and identified by the deuteration shift (−3 cm^{-1}) of 2-MeIm. Consequently, our previous assignment of the quaternary structure-sensitive Raman line of deoxyhemoglobin to the Fe(II)-N_ϵ(His F8) stretching mode was confirmed. The Fe(II)-N(2-MeIm) stretching band of Fe^{II}(PP)(2-MeIm) was shifted from 206 to 220 cm^{-1} when detergent was absent. The frequency change was attributed to interactions between 2-MeIm and solvent H_2O, on the basis of the data for variation of the 2-MeIm/Fe^{II}(PP) ratio. The Fe(II)-O_2 stretching frequency differed appreciably between solution and solid state, but differed little between $Fe^{II}(T_{piv}PP)(1,2\text{-}Me_2Im)O_2$ and $Fe^{II}(T_{piv}PP)$(1-MeIm)O_2 even in the solid state, although the former and latter are considered to be models of the T and R structures of hemoglobin. The ν_4 frequencies of $Fe^{II}(T_{piv}PP)(1,2\text{-}Me_2Im)$ and $Fe^{II}(T_{piv}PP)$-(1-MeIm) in the solid state as well as in solution were distinct in the deoxy state, whereas they were alike in the oxy state. Thus, the oxygen affinity was presumed to be determined primarily in the deoxy state.

Analysis of resonance Raman spectra (RRS) of hemoproteins has provided detailed structural information on heme and its immediate surroundings.[1-3] Some Raman lines in the 1200–1700 cm^{-1} region have been practically used to characterize physicochemical properties of the heme of various hemoproteins including cytochrome P-450,[4,5] horseradish peroxidase,[6-8] cytochrome c',[9,10] and cytochrome oxidase.[11-14] Assignments of such Raman lines were discussed based mainly on the normal coordinate treatments.[15-19] A more complete set of experimental data including the isotopic frequency shifts, symmetry assignments, and combination modes has been collected for octaethylporphinatonickel(II) [Ni(OEP)],[20] and the vibrational modes for the individual Raman lines have been elucidated by the subsequent normal coordinate calculations.[21] On the other hand, empirical correlations of the frequencies of selected Raman lines with the porphyrin core size[22,23] or with molecular species of axial ligands[24] have also been discussed for iron-porphyrin derivatives.

For most heme enzymes the sixth coordination position of heme iron is the binding site of a reacting molecule such as oxygen, while the fifth coordination position is occupied by an amino acid residue of protein, most often by an imidazole nitrogen of a histidine residue. The state of the two axial ligands and the nature of the Fe-ligand(axial) bonds are greatly involved in the biological functions of the protein. Therefore, the

* Address correspondence to this author at the Department of Molecular Physiological Chemistry, Medical School, Osaka University, Joan-cho, Kitaku, Osaka, 560, Japan.

0002-7863/80/1502-3608$01.00/0